ChemComm

Check for updates

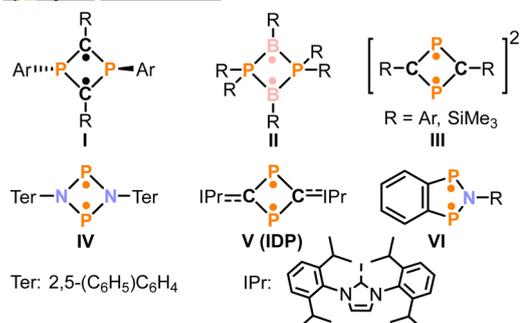# Redox-induced dimerisations of a phosphacyclic biradicaloid†

David Zuber,[a] Oksana Storcheva,[a] Karsten Paul Lüdtke, [iD][b] Leonidas Brunk[a] and Peter Coburger [iD] *[a]

Despite the first examples being isolated more than two decades ago, little is known about the redox chemistry of stable phosphacyclic biradicaloids. Here, we demonstrate that a biradicaloid featuring a diphosphaindenyl backbone is able to undergo both oxidation and reduction reactions. One-electron oxidation results in the formation of a dicationic cage compound structurally related to an isomer of hypostrophene ($C_{10}H_{10}$). Reduction of PPI^{Ph} with [$Co_2(CO)_8$] results in the formation of the bimetallic complex 2, which contains a bis(benzodiphosphole) ligand.

Biradicaloids are open-shell singlet species in which two spatially separated radical centers couple antiferromagnetically. Consequently, such species often exhibit high reactivity and are believed to be essential intermediates in bond breaking and making processes.[1] However, starting with the pioneering work of Niecke, a range of phosphacyclic biradicaloids was isolated.[2,3] Some selected members are shown in Fig. 1a.[4–9] Their accessibility enabled systematic reactivity studies,[3] as illustrated in Fig. 1b: As expected, such species function as biradicals, exemplified in the concerted addition of dihydrogen leading to secondary bis(phosphines) (**VII**).[7,8] Also, the radical centres can react independently.[10,11] This is demonstrated in the reactivity of **II** toward BrCCl$_3$ which involves two consecutive radical abstraction reactions leading to **VIII**. Additionally, biradicaloids can also act as charge-separated zwitterionic compounds as is, among others,[12,13] demonstrated by the isolation of gold complex **IX**. Recent studies have also revealed that phosphacyclic biradicaloids can serve as π-donating ligands, forming half-sandwich complexes such as **X**.[14–16] In these complexes, the biradicaloid ligands exhibit redox non-innocent behavior.[15,16] Compared to this rich follow-up

chemistry, the redox chemistry of phosphacyclic biradicaloids is somewhat limited. Notable examples are the reduction of **I** with an excess of lithium,[5] which yields **III** and the one-electron oxidations of **IV** and **IDP** (**V**) with ferrocenium and silver salts, resulting in the formation of radical cations **XI** and **XII**. Due to

[a] *Technical University of Munich, Department of Chemistry, Lichtenbergstr. 4, D-85747, Garching, Germany. E-mail: peter.coburger@tum.de*

[b] *University of Rostock, Institute of Chemistry, Albert-Einstein-Straße 3a, D-18059, Rostock, Germany*

† Electronic supplementary information (ESI) available. CCDC 2389673–2389675. For ESI and crystallographic data in CIF or other electronic format see DOI: https://doi.org/10.1039/d4cc05656f
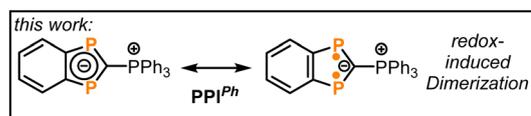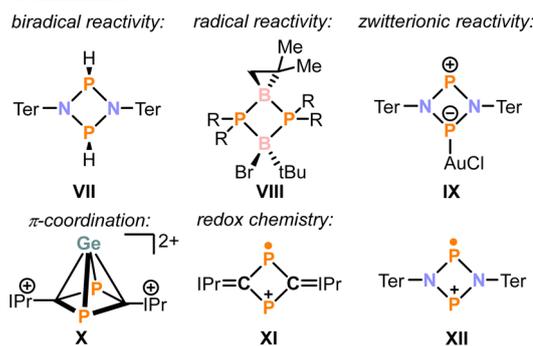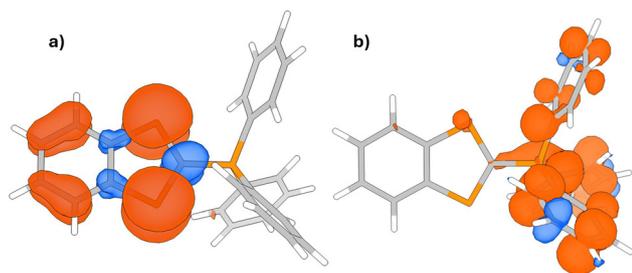

Fig. 1 (a) Selected examples of phosphacyclic biradicaloids; (b) reactivity of phosphacyclic biradicaloids. For clarity, only the biradical resonance structure of all biradicaloids is shown, except for **PPI**.

Fig. 2 Spin-density plots of [**PPI**^{Ph}]$^{\bullet+}$ (a) and [**PPI**^{Ph}]$^{\bullet-}$ (b).

Scheme 1 Redox chemistry of **PPI**^{Ph}. For a proposed mechanism on the formation of **2**, see Scheme 2.

the steric protection provided by their bulky substituents, these radical cations are stable and can be isolated. Based on these observations, we hypothesized that biradicaloids with reduced steric hindrance may serve as sources of radicals upon reduction or oxidation, which may undergo subsequent follow-up reactions.

Recently, we reported on the synthesis of **PPI**$^{p\text{-tol}}$, a phosphonium-substituted diphosphaindenylide exhibiting a notable biradical character (see Fig. 1a).[17] Here, the superscript denotes the substituents at the phosphonium moiety (p-tol: para-tolyl). A CV study revealed the presence of two irreversible redox events, an oxidation at $E = -0.30$ V and a reduction at $E = -2.95$ V vs. Fc/Fc$^+$ (peak potentials at a scan rate of 100 mV s^{-1}, [nBu$_4$N]PF$_6$ as electrolyte, THF).[17] Consequently, we identified **PPI** as an appropriate candidate for further investigation into the redox chemistry of phosphacyclic biradicaloids.

To get preliminary insights, the spin densities of the anticipated one-electron oxidation and reduction products [**PPI**]$^+$ and [**PPI**]$^-$ were calculated using the ORCA program package (Fig. 2, see the ESI,† for details).[18] These calculations highlight the zwitterionic nature of **PPI**: inspection of the spin-density plot and the Mulliken spin populations indicate that the one-electron oxidation of **PPI** primarily takes place at the endocyclic phosphorus atoms which carry a spin population of 0.45e and 0.47e, respectively. In contrast, the one-electron reduction is expected to occur at the cationic phosphonium moiety (Fig. 2b). With these DFT results in hand, we proceeded to investigate the chemical redox behaviour of **PPI**. Note that, as we encountered difficulties with crystallisations using the already reported **PPI**$^{p\text{-tol}}$, we prepared the phenyl-substituted derivative **PPI**^{Ph} to isolate and characterise the novel species in this study (see the ESI,† for the analytical data of **PPI**^{Ph}).

Indeed, treatment of **PPI**^{Ph} with one equivalent of ferrocenium tetrafluoroborate or triflate in polar solvents such as acetonitrile, THF or 1,2-dimethoxyethane (DME) results in the facile and selective formation of a novel polyphosphorus compound [**1**]$^{2+}$ as indicated by ^{31}P{1H} NMR spectroscopy (Scheme 1 and Fig. 3b, vide infra). Therefore, presumably due to the absence of significant steric shielding, the initially formed radical cation [**PPI**^{Ph}]$^+$ dimerises. The salts [**1**](OTf)$_2$· dme and [**1**](BF$_4$)$_2$·dme were obtained as colourless crystals in 59% or 90% yield, respectively. X-ray diffraction measurements revealed that [**1**]$^{2+}$ is a benzannulated C$_2$P$_4$ cage compound which consists of two **PPI**^{Ph} fragments fused via two C–P bonds and one P–P bond resulting (Fig. 3a). The P4–P5 distance in the
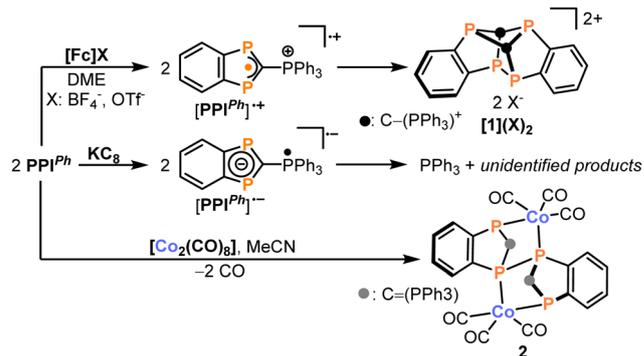
bicyclic C$_2$P$_4$ cage falls within the range expected for single bonds (2.248(1) Å). In contrast, the C–P distances correspond to elongated single bonds (ϕ_{C-P}: 1.91 Å).[19]

These values are similar to the ones observed in the tetraphosphabicyclo[2.1.1]hexane (^{t}BuC)$_2$(PR)$_4$ (P–P: 2.2334(6) Å, ϕ_{C-P}: 1.89 Å, R = Cl and Cy).[20] Additionally, the exocyclic C–P distances correspond to single bonds and are thus indicative of the cationic phosphonium character of the PPh$_3$ moieties (ϕ_{C-P}: 1.82 Å). Altogether, [**1**]$^{2+}$ is best described as a phosphonium-substituted tetraphospha-derivative of an isomer of hypostrophene (C$_{10}$H$_{10}$).[21] Notably, the related hexaphospha-derivative of this hypostrophene isomer was synthesised recently via the oxidation of the triphospholide [^{t}Bu$_2$C$_2$P$_3$]$^-$.[22]

In a CD$_2$Cl$_2$ solution, [**1**]$^{2+}$ is C_2-symmetric as indicated by the presence of three multiplets with an approximate integral ratio of 1:1:1 in the ^{31}P{1H} NMR spectrum. In line with DFT calculations, scalar couplings between the ^{31}P nuclei within the C$_2$P$_4$ cage are negligible, and thus only couplings to the exocyclic phosphonium moieties are observed (see the ESI†). This results in well-resolved first-order multiplets at 26.9 (P1, P6), 29.6 (P4, P5) and 45.7 (P2, P3) ppm (numbering according to Fig. 3a, see Fig. 3b for the respective coupling constants).

Having explored the oxidation chemistry of **PPI**^{Ph}, we shifted our focus to its reactivity toward reducing agents. Treatment of **PPI**^{Ph} with one equivalent of potassium graphite, KC$_8$, yields an intractable product mixture with triphenylphosphine being a major product (see the ESI†). Thus, in agreement with our DFT calculations, the reduction might take place at the phosphonium moiety resulting in the radical anion [**PPI**^{Ph}]$^-$. This radical species might decompose to PPh$_3$ and a diphosphaindenyl radical which then undergoes further unselective reactions. In light of these findings, we reasoned that a reductant capable of simultaneously acting as a coordinating agent might improve the selectivity of the reduction reaction by effectively trapping the generated radical anions. And indeed, treatment of **PPI**^{Ph} with [Co$_2$(CO)$_8$] leads to the formation of the bimetallic complex **2** as a yellow insoluble product which was isolated in 70% yield (Scheme 2). Single-crystal X-ray diffraction studies revealed the molecular structure of **2** (Fig. 3c): here, two **PPI**^{Ph} units are linked via a P–P single bond (P2–P2′: 2.248(2) Å) and the resulting dimeric ligand chelates two Co(CO)$_3$ units. Within

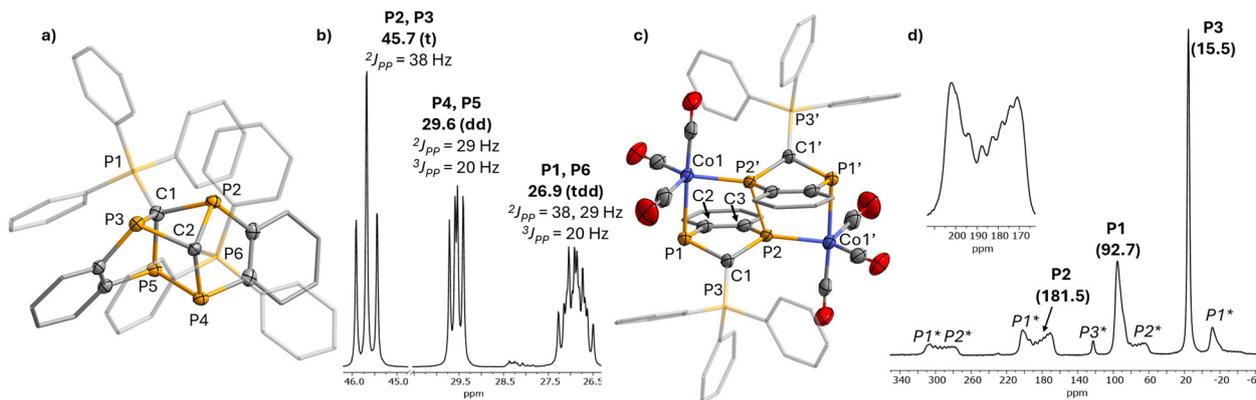**Fig. 3** (a) Solid-state structure of $[1]^{2+}$; (b) section of the $^{31}P\{^1H\}$ NMR spectrum of $[1](OTf)_2$ in CD_2Cl_2; (c) solid-state structure of **2**; (d) MAS ^{31}P solid-state NMR spectrum of **2** at a MAS frequency of 13.5 kHz, spinning side bands are marked with a star (*). For all solid-state structures, ellipsoids are drawn at the 50% probability level, hydrogen atoms and counterions are omitted for clarity and PPh_3 moieties and part of the indenyl systems are drawn as wireframe for clarity. Selected distances [Å]: $[1]^{2+}$: C1–P1 1.819(3), C1–P2 1.905(3), C1–P3 1.894(3), C1–P5 1.916(3), C2–P2 1.900(3), C2–P3 1.924(3), C2–P4 1.902(3), C2–P6 1.821(3), P4–P5 2.248(1); **2**: C1–P1 1.811(5), C1–P2 1.780(4), C1–P3 1.698(4), C2–P1 1.836(5), C3–P2 1.830(5), P2–P2′ 2.248(2), Co1–P1 2.468(2), Co1–P2′ 2.226(2).

the phosphorus ligand, all C–P distances correspond to single bonds (ϕ_{C-P}: 1.81 Å).[19]

In contrast to the oxidation product $[1]^{2+}$, the C–P bond formed between the C_3P_2 ring and the exocyclic PPh_3 moiety is a double bond indicating the presence of a neutral C=PPh_3 phosphorane moiety (C1–P3 1.698(4) Å).[23] Furthermore, the cobalt atoms in **2** adopt a trigonal-bipyramidal coordination environment with the phosphorus atoms occupying axial (P1, P1′) and equatorial positions (P2, P2′). The Co1–P2′ distance of 2.226(2) Å lies within the range typically found for Co–P single bonds in species with multiple Co–P bonds.[24–27] In contrast, the Co1–P1 distance is notably elongated with 2.468(2) Å, presumably due to the structural constraints provided by the chelating ligand. Due to its insolubility in common organic solvents, **2** was further characterised *via* elemental analysis, powder X-ray diffraction and magic-angle spinning (MAS) ^{31}P solid-state NMR spectroscopy (see the ESI,† for details). In line with the solid-state structure, the ^{31}P NMR spectrum shows three resonances at 15.5 (P3, P3′), 92.7 (P1, P1′) and 181.5 (P2, P2′) ppm (assigned using DFT calculations, see

the ESI,† for details). Notably, the coupling of the ^{59}Co nucleus to P2/P2′ is well-resolved (I = 7/2, 100% natural abundance, see the insert of Fig. 3d). After fitting, a coupling constant of $^1J_{P-Co}$ = −535 Hz was obtained, consistent with values observed in other cobalt carbonyl complexes with phosphine ligands (see the ESI†).[28,29] In the ATR-IR spectrum, **2** shows three intense CO stretching vibrations at 2017, 1973 and 1939 cm^{-1}. These values fall within the range reported for cobalt(I) carbonyl complexes with phosphine ligands.[30,31] Therefore, consistent with the assumption of a reduction of **PPI** during the reaction with cobalt carbonyl, the IR data allow to characterise **2** as a cobalt(I) complex with a chelating dianionic bis(benzodiphosphole)-diide ligand.

Further insight into the electronic structure of **2** was obtained from DFT and CASSCF calculations (see the ESI†). These calculations reveal a 3d^8 configuration of the cobalt centres together with dative P2′ → Co1 bonding interactions. The P–Co bonding orbitals involving P1/P1′ exhibit a high covalency and are formed by interaction of a p-type orbital on P1 and a d-type orbital on Co. This covalent bond is polarised toward P1 as indicated by the occupation of the p-type orbital of 1.27e (see the ESI,† for a detailed discussion). Thus, our calculations support a formal oxidation state of +1 for the cobalt centers in **2**.

The formation of **2** can be explained by the proposed mechanism outlined in Scheme 2 (see the ESI,† for details). Initially, the reaction between two equivalents of **PPI**^{Ph} and $[Co_2(CO)_8]$ might form the 19-valence electron complex **3** in an endergonic reaction (ΔG° = 7.9 kcal mol^{-1}). From there, loss of carbon monoxide generates the 17-valence electron complex **4** in an exergonic reaction (ΔG° = −15.7 kcal mol^{-1}). Two mesomeric resonance structures can be formulated to describe the electronic structure of **4** (Scheme 2). In **4a**, the unpaired electron is located at the cobalt centre making it a Co^0 complex. In contrast, **4b** is a Co^I complex with a reduced **PPI**^{Ph} ligand carrying an unpaired electron on the non-coordinated
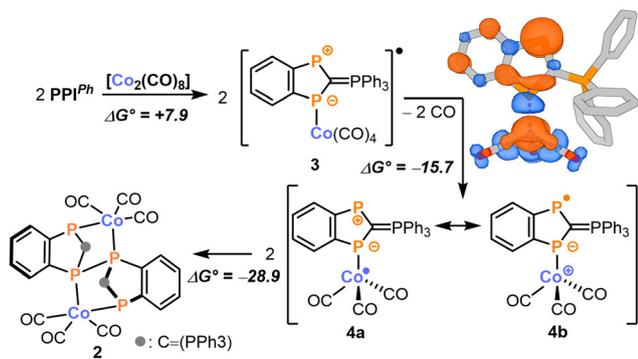
Scheme 2 Tentative mechanism for the formation of **2** together with the calculated spin density of **4** (top right corner). Energy values are given in kcal mol^{-1}.

endocyclic P atom (Scheme 2). The considerable spin population of 0.33e of this phosphorus atom indicates a substantial contribution of **4b** to the overall electronic structure of **4** (see Scheme 2 for a depiction of the spin density). Consequently, **4** can dimerise upon formation of a P–P single bond to form **2** in an exergonic reaction ($\Delta G^\circ = -28.9$ kcal mol^{-1}).

In summary, the zwitterionic structure of **PPI**^{Ph} promotes a diverse redox chemistry, *i.e.* facile one-electron oxidation and reduction reactions.

The lack of steric hindrance allows the initially generated radical species to undergo subsequent reactions. In the case of oxidation, this leads to the selective formation of $[\mathbf{1}]^{2+}$. In contrast, reduction with potassium graphite results in the unselective formation of multiple products. Gratifyingly, $[\text{Co}_2(\text{CO})_8]$ as reductant effectively redirects the reduction event to the C_2P_3 ring rather than to the phosphonium moiety leading to the formation of complex **2**, which features a reduced bis(benzodiphosphole) ligand. Therefore, using other bimetallic complexes for the reduction of **PPI**^{Ph} may yield a range of novel coordination compounds. Notably, the significant elongation of one Co–P bond in complex **2** suggests potential hemilabile behaviour, making it promising for catalytic applications. We are now focusing on improving the solubility of bimetallic complexes like **2** and to further assess their reactivity.

Data availability

The data supporting this article have been included as part of the ESI.†

Conflicts of interest

There are no conflicts to declare.

Notes and references

1 F. Breher, *Coord. Chem. Rev.*, 2007, **251**, 1007–1043.
2 W. W. Schoeller, *Eur. J. Inorg. Chem.*, 2019, 1495–1506.
3 A. Hinz, J. Bresien, F. Breher and A. Schulz, *Chem. Rev.*, 2023, **123**, 10468–10526.
4 E. Niecke, A. Fuchs, F. Baumeister, M. Nieger and W. W. Schoeller, *Angew. Chem., Int. Ed. Engl.*, 1995, **34**, 555–557.
5 M. Sebastian, M. Nieger, D. Szieberth, L. Nyulászi and E. Niecke, *Angew. Chem., Int. Ed.*, 2004, **43**, 637–641.
6 D. Scheschkewitz, H. Amii, H. Gornitzka, W. W. Schoeller, D. Bourissou and G. Bertrand, *Science*, 2002, **295**, 1880–1881.
7 T. Beweries, R. Kuzora, U. Rosenthal, A. Schulz and A. Villinger, *Angew. Chem., Int. Ed.*, 2011, **50**, 8974–8978.
8 Z. Li, X. Chen, D. M. Andrada, G. Frenking, Z. Benkö, Y. Li, J. R. Harmer, C.-Y. Su and H. Grützmacher, *Angew. Chem., Int. Ed.*, 2017, **56**, 5744–5749.
9 J. Bresien, D. Michalik, A. Schulz, A. Villinger and E. Zander, *Angew. Chem., Int. Ed.*, 2021, **60**, 1507–1512.
10 H. Amii, L. Vranicar, H. Gornitzka, D. Bourissou and G. Bertrand, *J. Am. Chem. Soc.*, 2004, **126**, 1344–1345.
11 J. Rosenboom, L. Chojetzki, T. Suhrbier, J. Rabeah, A. Villinger, R. Wustrack, J. Bresien and A. Schulz, *Chem. – Eur. J.*, 2022, **28**, e202200624.
12 A. Hinz, A. Schulz and A. Villinger, *Chem. Commun.*, 2016, **52**, 6328–6331.
13 Z. Li, Y. Hou, Y. Li, A. Hinz and X. Chen, *Chem. – Eur. J.*, 2018, **24**, 4849–4855.
14 Z. Li, X. Chen, L. L. Liu, M. T. Scharnhölz and H. Grützmacher, *Angew. Chem., Int. Ed.*, 2020, **59**, 4288–4293.
15 M. T. Scharnhölz, P. Coburger, L. Gravogl, D. Klose, J. J. Gamboa-Carballo, G. Le Corre, J. Bösken, C. Schweinzer, D. Thöny, Z. Li, K. Meyer and H. Grützmacher, *Angew. Chem., Int. Ed.*, 2022, **61**, e202205371.
16 P. Coburger, F. Masero, J. Bösken, V. Mougel and H. Grützmacher, *Angew. Chem., Int. Ed.*, 2022, **61**, e202211749.
17 P. Coburger, D. Zuber, C. Schweinzer and M. Scharnhölz, *Chem. – Eur. J.*, 2024, **30**, e202302970.
18 F. Neese, F. Wennmohs, U. Becker and C. Riplinger, *J. Chem. Phys.*, 2020, **152**, 224108.
19 F. H. Allen, O. Kennard, D. G. Watson, L. Brammer, A. G. Orpen and R. Taylor, *J. Chem. Soc., Perkin Trans. 2*, 1987, S1–S19.
20 C. Jones, P. C. Junk, A. F. Richards and M. Waugh, *New J. Chem.*, 2002, **26**, 1209–1215.
21 B. M. Gimarc and M. Zhao, *J. Org. Chem.*, 1995, **60**, 1971–1974.
22 M. K. Uttendorfer, G. Hierlmeier, G. Balázs and R. Wolf, *Dalton Trans.*, 2024, **53**, 10113–10119.
23 R. Appel, *Pure Appl. Chem.*, 1987, **59**, 977–982.
24 D. M. Jenkins and J. C. Peters, *J. Am. Chem. Soc.*, 2005, **127**, 7148–7165.
25 P. Coburger, S. Demeshko, C. Rödl, E. Hey-Hawkins and R. Wolf, *Angew. Chem., Int. Ed.*, 2017, **56**, 15871–15875.
26 P. Coburger, J. Leitl, D. J. Scott, G. Hierlmeier, I. G. Shenderovich, E. Hey-Hawkins and R. Wolf, *Chem. Sci.*, 2021, **12**, 11225–11235.
27 R. Franz, D. Gál, C. Bruhn, Z. Kelemen and R. Pietschnig, *Adv. Sci.*, 2024, **11**, 2306805.
28 D. Massiot, F. Fayon, M. Capron, I. King, S. Le Calvé, B. Alonso, J.-O. Durand, B. Bujoli, Z. Gan and G. Hoatson, *Magn. Reson. Chem.*, 2002, **40**, 70–76.
29 G. Szalontai, in *Current Developments in Solid State NMR Spectroscopy*, ed. N. Müller and P. K. Madhu, Springer, Vienna, 2003, pp. 95–106.
30 P. Rigo, M. Bressan and A. Morvillo, *J. Organomet. Chem.*, 1976, **105**, 263–269.
31 H. Schumann, M. Meissner and H.-J. Kroth, *Z. Naturforsch., B*, 1978, **33**, 1489–1490.